Applied Catalysis B: Environmental 180 (2016) 13–19

Contents lists available at ScienceDirect

Applied Catalysis B: Environmental

journal homepage: www.elsevier.com/locate/apcatb

Preparation of hollow multiple-Ag-nanoclustes-C-shell nanostructures and their catalytic properties

Wenjun Dong[a,b,*], Longfei Zhang[a], Baozhen Li[a], Lina Wang[a], Ge Wang[b,**], XiaoYun Li[a], Benyong Chen[a], Chaorong Li[a]

[a] Center for Nanoscience and Nanotechnology, Zhejiang Sci-Tech University, Hangzhou 310018, China
[b] Beijing Key Laboratory of Function Materials for Molecule & Structure Construction, School of Materials Science and Engineering, University of Science and Technology Beijing, Beijing 100083, PR China

ARTICLE INFO

Article history:
Received 9 February 2015
Received in revised form 30 May 2015
Accepted 31 May 2015
Available online 4 June 2015

Keywords:
Ag nanoclusters
C shell
Hollow nanostructures
Catalytic properties

ABSTRACT

Hollow multiple-Ag-nanoclustes-C-shell nanostructures containing stabilized Ag nanocluster and hollow C shell were successfully fabricated from well-defined Ag@C core–shell templates via a simultaneous synthesis and assembly strategy. The core–shell Ag@C templates were hydrothermally achieved using glucose and silver nitrate reactants, and the glucose served as mild reducing agent for reducing Ag^+ to Ag and as carbon source for generating C shells with active groups, simultaneously. Then the hollow multiple-Ag-nanoclustes-C-shell nanostructures were fabricated by a redox reaction between the Ag@C templates and H_2O_2. H_2O_2 played a role of smart etchant in controlling dissolving and oxidizing the initial Ag cores to Ag^+ anions. During such transformation process, Ag^+ was firstly diffused from Ag core to C shell and then reduced into Ag nanoclusters by the active groups in the C shell. The dispersion, particle size and the arrangement of Ag nanoclusters in the C shell depended heavily on the processing time. The hollow multiple-Ag-nanoclustes-C-shell nanostructures exhibit an excellent catalytic activity and recyclability for the reduction of *p*-nitrophenol due to their small size, high dispersion, and high number density of the Ag nanoclusters on the C shell.

1. Introduction

In general, nanometer-size metallic particles possess high surface-to-volume ratio [1–3], which contribute significantly to their outstanding physical [4,5], chemical [6–10] and biological [11,12] properties. However, it is essential to achieve desirable dispersion of smaller metal nanoparticles (NPs) to exploit their functions to the greatest degree, which otherwise will be jeopardized by aggregation of the particles [13–16]. Recently, the interest toward the hierarchical hybrid nanostructures, especially highly dispersed metal particles in functional matrix, has continuously increased due to their unique structures and excellent properties [17–22]. For instance, highly dispersed nanoparticles in/on a matrix with a well-defined pore structure often result in enhanced catalytic activity and stability [23–26]. In particular, carbon sphere matrix can serve as shell/cover to trap up active Ag NPs and effectively prevent their agglomeration even though the NPs present a high particle-density in the matrix [27]. Moreover, outer surface of the C shell provides numerous convenient channels to facilitate diffusion and transport of reactants to reach the surface of the active cores, i.e., Ag NPs [28].

Such kind of core/shell nanostructures offer protection to the metal cores [29–32] and are more conveniently to be separated and recycled [33] in terms of catalytic applications. New functionalities can be introduced into these hybrid core/shell nanostructures, which generate a possibility to combine the advantages or distinctive properties of various materials [34]. So far, numerous core/shell nanoparticles have been developed. For instance, Lu and co-workers synthesized a stable dispersion of Au@SiO_2 core/shell colloids [35]. Sun et al. reported the preparation of Ag@C core/shell nanoparticles with organic-group-loaded surfaces, which improved the hydrophilicity and stability of the microspheres in aqueous systems [36]. Liu and co-workers prepared Ag@C nanostructures by using an extended Stöber method involving simultaneous reduction of $AgNO_3$ and the carbonization of the resorcinol-formaldehyde-resin [37]. Hollow Ag@SiO_2 spheres were

* Corresponding author at: Center for Nanoscience and Nanotechnology, Zhejiang Sci-Tech University, Hangzhou 310018, China. Tel.: +86 10 62333827; fax: +86 10 62333827.
** Corresponding author.
E-mail addresses: wdong@ustb.edu.cn (W. Dong), gewang@mater.ustb.edu.cn (G. Wang).

http://dx.doi.org/10.1016/j.apcatb.2015.05.061
0926-3373/

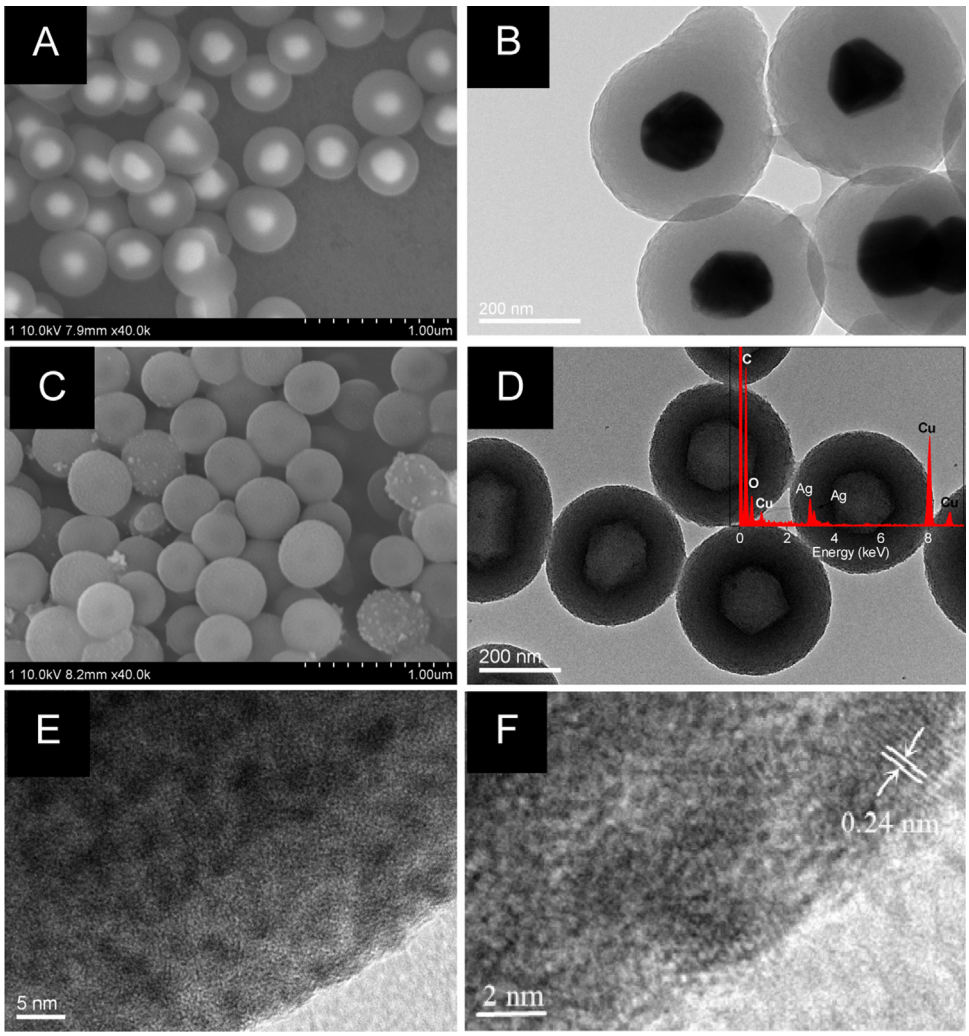

Fig. 1. SEM and TEM images of (A and B) Ag@C core–shell nanostructures and (C–F) hollow multiple-Ag-nanoclusters-C-shell nanostructures. EDS spectrum (the inset of D) of the hollow multiple-Ag-nanoclusters-C-shell nanostructures.

also fabricated to enhance catalytic activity and stability of Ag NPs [38]. Tang et al. developed a microwave-hydrothermal method to dope Ag NPs in monodispersed C spheres, which exhibited excellent catalytic activity toward the reduction of *p*-nitrophenol by sodium borohydride [39]. There are many advantages of designing appropriate shell materials in core/shell structure, such as improving the functionality stability and dispensability of the composite, reducing the consumption of precious materials, and so on [40]. The property of these nanoparticles depends greatly on their size, structure, morphology, dispersion, and chemical physical environment. However, dimension and density control of the Ag NPs in/on C matrix for efficient catalytic reaction remain a challenge.

In this paper, a simple route toward synthesis of highly dispersed Ag nanoclusters on hollow C shell was developed. Firstly, Ag@C core–shell nanostructure was prepared by reducing $AgNO_3$ in a glucose solution that was used as reducing agent to transform Ag^+ to Ag core and also played as carbon source for the C shell. Then the Ag@C nanostructure reacted with H_2O_2, and the Ag core with a diameter of about 120 nm was gradually dissolved into Ag nanoclusters, which were then wrapped up by the C shell. H_2O_2, acting as a smart oxidation agent, can oxidize the initial Ag core to Ag^+. On the other hand, the decomposition of H_2O_2 into O_2 gas bubble provided the driving force to push Ag^+ ions moving toward the C shell. Subsequently, the active groups in the amorphous C shell reduced Ag^+ to small Ag nanoclusters in situ, which also improved the dispersion and separation of Ag nanoclusters in/on the C shell. The hollow multiple-Ag-nanoclustes-C-shell nanostructures exhibited a highly catalytic activity in the reduction of *p*-nitrophenol due to the small size, high dispersion, and high number-density of the Ag nanoclusters on the C shell.

2. Experimental

2.1. Preparation of Ag@C core–shell nanostructures

Ag@C core–shell nanostructures were synthesized by a hydrothermal method according to the previous report [41]. In a typical procedure, 1.0 g of glucose ($C_6H_{12}O_6{\cdot}H_2O$) was added to 20 mL of de-ionized water under vigorous magnetic stirring for 10 min, and 0.5 mL of $AgNO_3$ (0.1 M) was added into the solution and stirred for another 10 min and then transferred into a Teflon-lined autoclave (30 mL in volume). The Teflon-lined autoclave was sealed and maintained at 180 °C for 3 h. Then the autoclave was naturally cooled down to room temperature and the Ag@C core–shell composites were collected by centrifugation and washed with water and ethanol alternately, for 3 times. As-prepared Ag@C product was dried at 60 °C in air overnight.

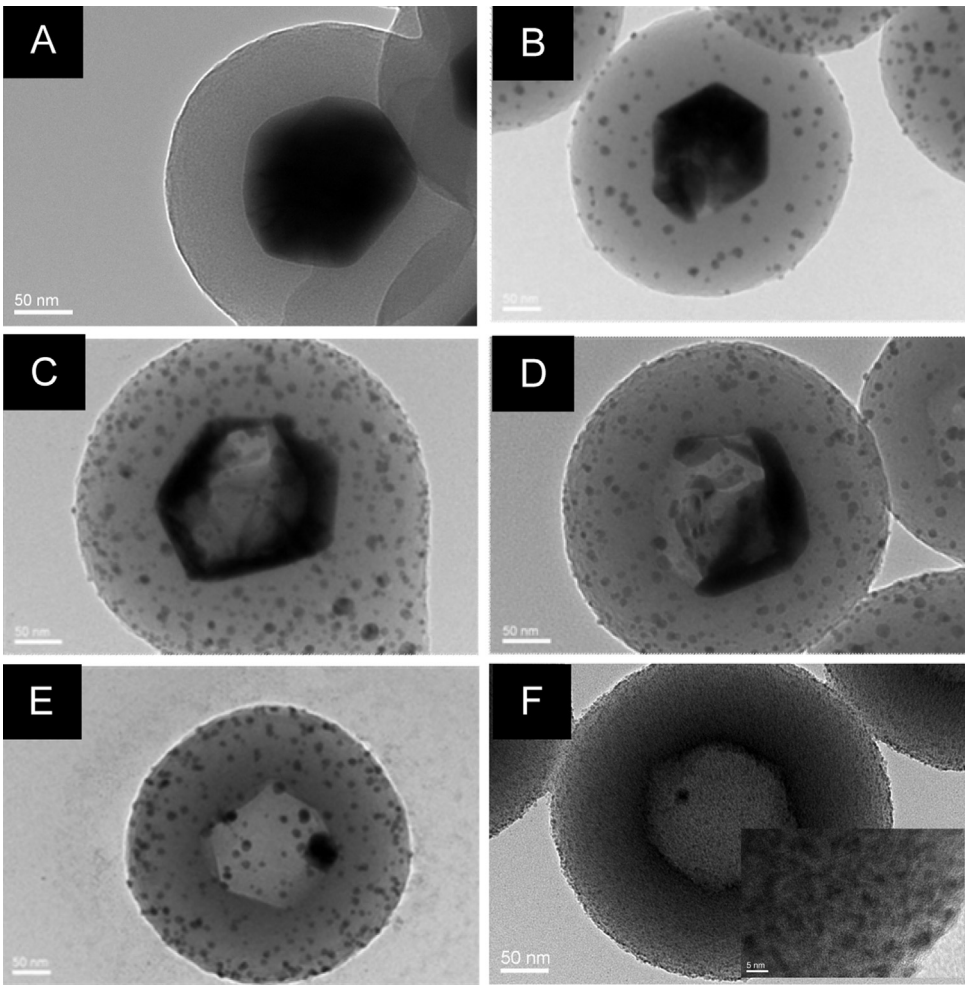

Fig. 2. TEM images of products at varied time reacting with hydrogen peroxide: (A) 0 min; (B) 10 min; (C) 20 min; (D) 30 min; (E) 60 min; and (F) 120 min. The inset of F shows the corresponding HRTEM image.

2.2. Preparation of hollow multiple-Ag-nanoclustes-C-shell nanostructures

Ag@C core–shell nanostructures were dispersed in 50 mL of deionized water and followed by addition of 2 mL of H_2O_2 (36% mass fraction). The solution was then stirred for 120 min at 0 °C in an ice bath. The solid product was collected by centrifugation and washed with water and ethanol for 3 times. The final hollow multiple-Ag-nanoclustes-C-shell products was prepared and dried at 60 °C in air overnight.

2.3. Catalytic property of the hollow multiple-Ag-nanoclustes-C-shell nanostructures

The hollow multiple-Ag-nanoclustes-C-shell nanostructure catalyst was added into 2.8 mL of *p*-nitrophenol aqueous solution (5.0×10^{-5} M) under continuous stirring. A freshly prepared aqueous solution of $NaBH_4$ (0.20 mL, 0.1 M) was then added. The progress of the conversion reaction was monitored by recording time-dependent UV–vis absorption spectra of the mixture using a spectrophotometer with wavelength over the range of 275–600 nm. The catalytic activity of the Ag@C core–shell nanostructure was also carried out under the similar reaction conditions for comparison with the case of the hollow multiple-Ag-nanoclusters-C-shell nanostructures.

2.4. Characterizations

X-ray diffraction (XRD) patterns were obtained on a Bruker D8 Advance X-ray diffractometers uing Cu Kα radiation with a scanning step scanning of 0.02 °s^{-1} at room temperature. The morphology and size of products were characterized on a field emission scanning electron microscope (FESEM, Hitachi S-4800) and a transmission microscope (TEM, JEOL, JEM-2100, 200 kV), combined with an energy-dispersive X-ray spectroscope (EDS) for determination of chemical composition. The nitrogen adsoption–desorption isotherms were measured on a Micromeritics ASAP 2020 accelerated surface area analyzer. FT-IR spectra were recorded on a Nicolet Nexus spectrometer with the standard KBr pellet method. The catalytic properties of the products were investigated by a UV–vis absorption (UNICO, UV-4802H) spectrometer.

3. Results and discussion

3.1. Characterization of structure and morphology

As-prepared Ag@C compound displayed a typical core/shell structure with excellent dispersion (Fig. 1A). In terms of the Ag@C core–shell nanostructure, the atomic number of Ag is greater than that of C, which leads to a bright Ag core and a dark C shell under SEM observation [42,43]. Ag core was about 120 nm in diameter and C shell was about 100 nm in thickness (Fig. 1B).

When the Ag@C hybrids reacted with H_2O_2 for a time period of 120 min, the core/shell structure was perfectly preserved (Fig. 1C). It was worthwhile pointing out that the Ag core was dissolved gradually into a number of smaller Ag nanoclusters, and then dispersed into the C shell. After a complete dissolution of the Ag core, a cavity appeared (Fig. 1D) and the hollow multiple-Ag-nanoclusters-C-shell nanostructure was finally obtained. EDS spectrum of the hollow multiple-Ag-nanoclusters-C-shell nanostructure reveals that C, copper (Cu), Ag, and oxygen (O) elements were present (inset Fig. 1D), and the Cu elements came from the TEM grid support [44]. HRTEM images (Fig. 1E) illustrates that a large number of Ag nanoclusters with a diameter of about 5 nm were homogeneously incorporated in the C shell and anchored on the surface of the shell. The lattice distance of the Ag nanocluster is approximately 0.24 nm, which is consistent with that of Ag (1 1 1) plane (Fig. 1F). The Ag nanoclusters were separated by C shells and were still well dispersed, where majority of the Ag NPs were isolated at high-volume fractions of Ag in C. As such, well-dispersed Ag nanoclusters located in and anchored on the surface of the hollow C sphere were successfully created without additional dispersing or stabilizing agent.

Size and density of the Ag nanoclusters could be systematically controlled by adjusting the reaction time. Fig. 2 demonstrates the evolution of the Ag@C core–shell nanostructure into the hollow multiple-Ag-nanoclusters-C-shell nanostructures. Initially, the Ag@C core–shell nanostructure templates were prepared by a hydrothermal method [36]. The hexahedron Ag core was set in the centre of the sphere and C was the sole component of the exterior shell material (Fig. 2A). Glucose was employed to reduce Ag^+ into Ag core and as carbon source to generate C shell structure. Then the Ag@C core–shell nanostructures were reacted with H_2O_2. After 10 min, Ag core was dissolved and a few smaller Ag nanoclusters about 10 nm in diameter were produced in the C shell whilst O_2 bubbles emerging (Fig. 2B). When the reaction was prolonged to 20 min, Ag core was partially dissolved and the Ag nanoclusters gradually appeared in the C shells (Fig. 2C). When the reaction time was continued for up to 30 min, a larger quantity of Ag nanoclusters were generated in the C shell (Fig. 2D) with a decrease in the diameter of the Ag core. When the reaction was prolonged to 60 min, the majority of the Ag core was dissolved and cavity space appeared (Fig. 2E). In the case of 120 min reaction, the Ag core nearly disappeared and the highly dispersed Ag nanoclusters were in/on the C shell (Fig. 2F). HRTEM image (inset Fig. 2F) reveals that the size of the Ag nanoclusters anchored on the surface of the C shell is about 5 nm.

Fig. 3 illustrates the XRD patterns of the Ag@C core–shell nanostructure, and the Ag@C core–shell nanostructure reacting with H_2O_2 for 30 min and 120 min, respectively. The main reflections located at 38.1°, 44.3°, 64.4° and 77.3° can be assigned to (1 1 1), (2 0 0), (2 2 0) and (3 1 1) planes of the face-centered cubic of Ag crystal (JCPDS card No. 04-0783). XRD pattern confirms the existence of the face-centered cubic (fcc) Ag in all products. After the Ag@C core–shell nanostructure were transformed into the hollow multiple-Ag-nanoclusters-C-shell nanostructures, the full width at half-maximum of XRD peak at 38.1° was obviously broadened (Fig. 3), indicating the average sizes of the Ag nanocluster in the C shell getting smaller. Moreover, according to the Scherrer Formula [45], the average size of the Ag cluster is about 5 nm in the hollow multiple-Ag-nanoclusters-C-shell nanostructure, which is in agreement with the TEM results (Fig. 2).

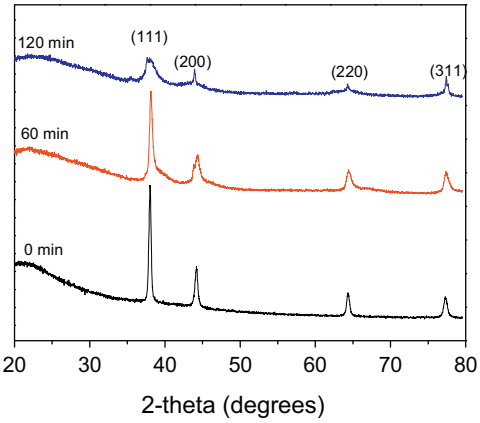

Fig. 3. XRD patterns of the hollow multiple-Ag-nanoclusters-C-shell nanostructures obtained by various time durations.

FT-IR spectrum of the Ag@C core–shell nanostructure is depicted in Fig. 4A, which clearly demonstrates the existence of the functional groups in the C shell. The characteristic peaks at 1710 and 1620 cm^{-1} (Fig. 4A) correspond to C=O and C=C vibrations, respectively, which can be attributed to the aromatization of glucose during the hydrothermal treatment [36]. The peaks in the range of 1000–1300 cm^{-1} include C—OH stretching and —OH bending vibrations, which implies the existence of large numbers of residual —OH groups. In general, partially dehydrated residues such as reductive aldehyde groups (CHO) and hydroxy groups (OH) are covalently bonded to the C frameworks [36], which can reduce the Ag^+ to Ag. It should be noted that the hydroxyl groups covalently bonded to the C frameworks are retained in the hollow multiple-Ag-nanoclusters-C-shell and can improve the hydrophilicity of the nanostructures [46]. Furthermore, the C shell of the hollow multiple-Ag-nanoclusters-C-shell nanostructures can control the density of the composites, which improves the stability of the hollow multiple-Ag-nanoclusters-C-shell nanostructures in aqueous systems, even in water for 2 h (inset Fig. 4A).

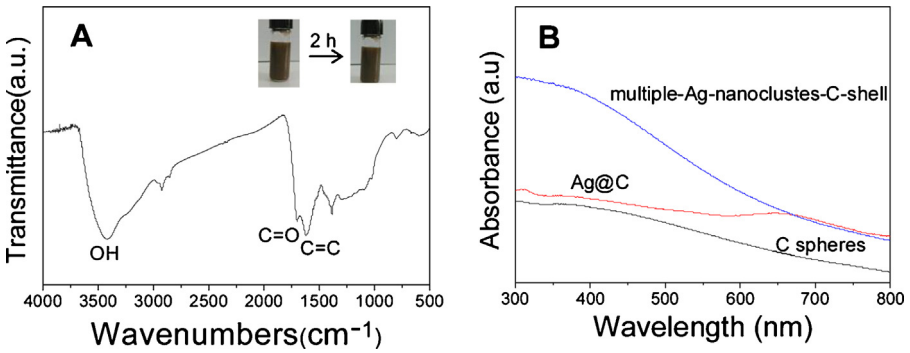

Fig. 4. FT-IR spectrum of the Ag@C core–shell nanostructure (A) and UV–vis absorption spectra of C spheres, Ag@C core–shell nanostructures and the hollow multiple-Ag-nanoclusters-C-shell nanostructures (B).

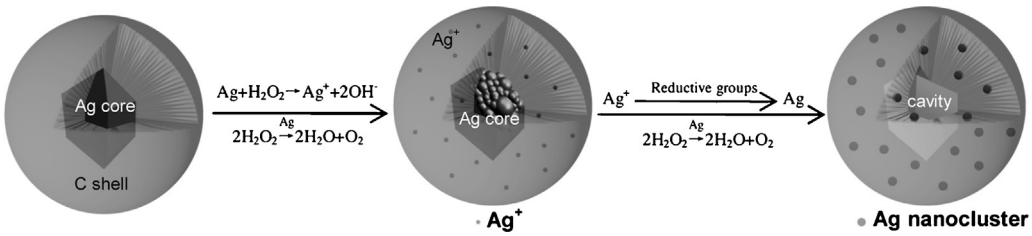

Scheme 1. Schematic demonstration of the preparation of the hollow multiple-Ag-nanoclusters-C-shell nanostructures.

Fig. 4B illustrates UV–vis spectra of C spheres [47], Ag@C core–shell nanostructures and the hollow multiple-Ag-nanoclusters-C-shell composites. No protruding absorption peak can be observed in the bare C sphere product. The Ag@C core–shell nanostructures presented wide absorption over the range of 300–800 nm. When the Ag@C core–shell templates were upgraded to hollow multiple-Ag-nanoclusters-C-shell nanostructures, the overall absorption was increased over a wide range from 300 to 800 nm, which can be attributed to the dipole–dipole coupling between neighboring metal NPs [39].

3.2. Formation mechanism of the hollow multiple-Ag-nanoclusters-C-shell nanostructures

On the basis of the morphological evolution of the time-dependent experiment results, the intrinsic growth mechanisms of the hollow multiple-Ag-nanoclusters-C-shell nanostructures were proposed (Scheme 1). Comparing the electrochemical potential $\phi_{H2O2/OH^-} = 0.867$ V with the $\phi_{Ag+/Ag} = 0.7996$ V [48] in the experimental conditions, H_2O_2 can oxidize Ag core to Ag^+. Interestingly, Ag catalyzes the decomposition of H_2O_2 to produce O_2 bubbles ($H_2O_2 \rightarrow H_2O + O_2\uparrow$ [49]), which can provide an outward driving force to induce Ag^+ diffusion in the C shell during the oxidization process of the Ag core into Ag^+. H_2O_2 was selected as an environmentally-friendly and effective etchant to etch the Ag core of the Ag@C core–shell template. The evolution from Ag@C core–shell nanostructure to the hollow multiple-Ag-nanoclusters-C-shell nanostructures includes the dissolution of Ag core to Ag^+ and the reduction of Ag^+ to Ag nanoclusters in the C shell. Firstly, the C shell provides channels for the infiltration of H_2O_2 into the C shell and the intermediate Ag core is oxidized to Ag^+ ($2Ag + H_2O_2 = 2Ag^+ + 2OH^-$ $\Delta E^0 = 0.067$ V) [48]. Simultaneously, the Ag can catalyze the decomposition of H_2O_2 to produce O_2 bubbles [49], and the O_2 bubbles drive the Ag^+ diffusing from core to shell and promote the silver ions dispersed in the C shell. Secondly, the diffused Ag^+ into the C shell is reduced in situ to disperse Ag nanoclusters by the active groups in the C shell. Then the hollow multiple-Ag-nanoclusters-C-shell nanostructures are produced. On the other hand, the Ag@C spheres and hollow multiple-Ag-nanoclusters-C-shell nanostructures both exhibited non-porous structures, and the corresponding BET surface area is increased from 11.6 m^2/g to 85.60 m^2/g (Fig. 5), which indicates the generation of O_2 during the Ag^+ reduction could generate some channels for the hollow multiple-Ag-nanoclusters-C-shell nanostructures. The average channel diameter of the hollow multiple-Ag-nanoclusters-C-shell nanostructures is about 13.0 nm. As a consequence, these channels could allow organic molecules easily access to the Ag nanoclusters on the surface of the carbon shell, resulting in an enhanced catalytic activity for organic reactions.

3.3. Catalytic properties of the hollow multiple-Ag-nanoclusters-C-shell nanostructures

Reduction of *p*-nitrophenol to *p*-aminophenol by $NaBH_4$ was employed as a model to evaluate catalytic activity of the hollow multiple-Ag-nanoclusters-C-shell nanostructures. The Ag nanoclusters on the C shell served as electron medium in the system for redox reactions. Usually, Ag nanoclusters exhibit attractive catalytic properties and the C shell can stabilize the Ag nanoclusters [27]. The outstanding catalytic activity of the hollow multiple-Ag-nanoclusters-C-shell nanostructures is attributed to the highly dispersed Ag nanoclusters on the C surface with a small size, high dispersion, and high number density. The conversion of *p*-nitrophenol was monitored by UV/Vis spectrometry, recording the change of its characteristic absorbance at $\lambda = 400$ nm in alkaline solution. The absorption peak of *p*-nitrophenol was shifted from 400 to 300 nm immediately, indicating the reduction of *p*-nitrophenol and formation of *p*-aminophenol, respectively. The reaction could not take place without catalyst, which has been reported by the previous studies [50]. When the hollow multiple-Ag-nanoclusters-C-shell was applied as catalyst (shown in Fig. 2D), the time-dependent absorption spectra shows a decrease in the intensity of the absorption peak at 400 nm and concomitant development of a new peak at 300 nm corresponding to *p*-aminophenol (Fig. 6A). The linear correlation between $\ln(C_t/C_0)$ and reaction time confirm that the reduction was catalyzed by the hollow multiple-Ag-nanoclusters-C-shell nanostructures and Ag@C core–shell was

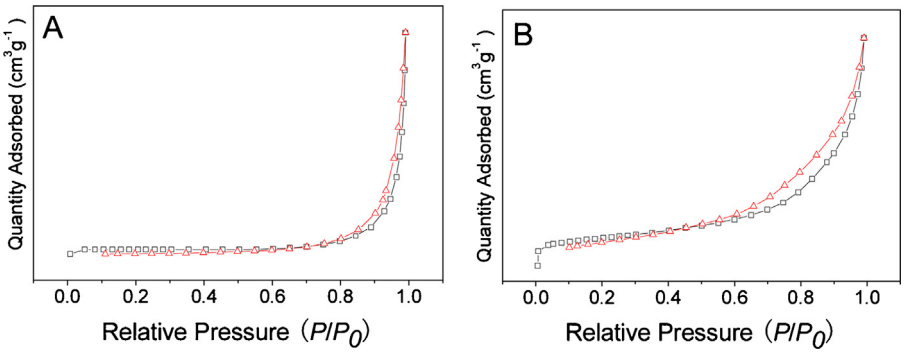

Fig. 5. Nitrogen-adsorption–desorption isotherm of (A) the Ag@C core–shell nanostructures, and (B) the hollow multiple-Ag-nanoclusters-C-shell nanostructures.

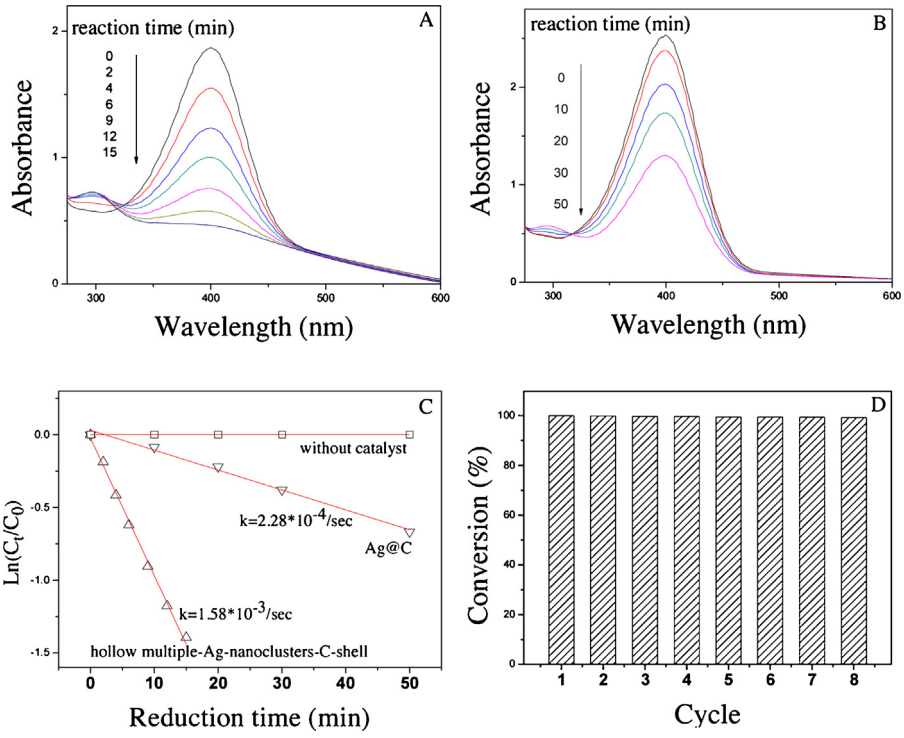

Fig. 6. Successive UV–vis absorption spectra (A and B) of the reduction of *p*-nitrophenol by $NaBH_4$ in the presence of the hollow multiple-Ag-nanoclusters-C-shell nanostructures and Ag@C core–shell nanostructure; (C) $\ln(C_t/C_0)$ versus reaction time for the reduction, no catalyst, Ag@C, hollow multiple-Ag-nanoclusters-C-shell nanostructures and (D) catalytic activity of the hollow multiple-Ag-nanoclusters-C-shell nanostructures for *p*-nitrophenol with eight times of cycling uses.

regarded as the first order reaction (Fig. 6C). When the hollow multiple-Ag-nanoclusters-C-shell nanostructure was used as catalyst, the reaction rate constant k was 1.58×10^{-3}/sec (Fig. 6C). In regards to the catalytic effect of the Ag@C core–shell, the *p*-nitrophenol solution concentration was degraded 52% (Fig. 6B) after 50 min. Previous reports confirmed that the ratios between rate constants k and the weight of catalyst are $0.09\,s^{-1}g^{-1}$ and $0.014\,s^{-1}g^{-1}$ for pure Ag NPs and Ag-NP-doped hollow poly (*N*-isopropylacrylamide) spheres, respectively [51]. The ratio of k over the weight of the hollow multiple-Ag-nanoclusters-C-shell nanostructures is $1.58\,s^{-1}g^{-1}$ in this work. The good catalytic activity of the hollow multiple-Ag-nanoclusters-C-shell nanostructures was attributed to the highly dispersed and small-sized Ag nanoclusters and their stable anchoring on the surface of C shell [52]. A large number of isolated and dispersed Ag nanoclusters on the surface of the C shell offered numerous interfaces, meanwhile, the channels derived from the C shell ensured the accessibility of reactant molecules to the active Ag nanoclusters surface.

The recyclability of the hollow multiple-Ag-nanoclusters-C-shell catalysts is revealed in Fig. 6D. After each reaction cycle, the catalysts were separated by centrifugation and reused for a consecutive run under the same reaction conditions. The hollow multiple-Ag-nanoclusters-C-shell catalyst remained substantially active over 8 recycles, and the conversion of *p*-nitrophenol was 93% (Fig. 6D). It demonstrates that the hollow multiple-Ag-nanoclusters-C-shell nanostructures were capable for efficient in catalytic hydrogenation reaction for long-lasting and recycle usage.

4. Conclusions

Hollow multiple Ag nanoclusters-C shell nanostructures were fabricated through a simple solution method, including synthesis of Ag@C core–shell nanostructures, dissolution of Ag core and the formation of Ag nanoclusters in/on the C shell. The metallic Ag core was dissolved and oxidized to Ag^+ anions during the reaction between Ag@C core–shell nanostructures and H_2O_2. Ag^+ anions diffused from Ag core into C shell and then in situ reduced to Ag nanoclusters by the active groups in the C shell. Ag nanoclusters in/on the C shell were achieved without additional dispersing or stabilizing agent. The robust hollow multiple-Ag-nanoclusters-C-shell nanostructures catalysts displayed a great catalytic activity in reduction of *p*-nitrophenol by sodium borohydride due to the isolated and highly dispersed Ag nanoclusters with numerous reaction interfaces. Controllable size and monodisperse Ag nanoparticles in matrix exhibit excellent properties and thereby could inspire intensive future research in this area.

Acknowledgments

This work was supported by the National Natural Science Foundation of China (No. 51272235, 51436001); National High-tech R&D Program of China (2013AA031702); Program forNew Century Excellent Talents in University (NCET-13-0998); Fundamental Scientific Research Funds for the Central Universities (230201406500016); Zhejiang Provincial Natural Science Foundation of China (LR12E02001); Program for Changjiang Scholars and Innovative Research Team in University (PCSIRT13097).

References

[1] T. Uemura, M. Ohba, S. Kitagawa, Inorg. Chem. 43 (2004) 7339–7345.
[2] K. Mori, A. Kumami, M. Tomonari, H. Yamashita, J. Phys. Chem. C 113 (2009) 16850–16854.
[3] K. Zhou, Y. Li, Angew. Chem. Int. Ed. 51 (2012) 602–613.
[4] P. Tartaj, T. González-Carreño, C.J. Serna, Langmuir 18 (2002) 4556–4558.
[5] S. Panigrahi, S. Praharaj, S. Basu, S.K. Ghosh, S. Jana, S. Pande, T. Vo-Dinh, H. Jiang, T. Pal, J. Phys. Chem. B 110 (2006) 13436–13444.
[6] P.D. Cozzoli, T. Pellegrino, L. Manna, Chem. Soc. Rev. 35 (2006) 1195–1208.
[7] K.M. Abou El-Nour, A. Eftaiha, A. Al-Warthan, R.A. Ammar, Arabian J. Chem. 3 (2010) 135–140.
[8] Y. Mei, Y. Lu, F. Polzer, M. Ballauff, M. Drechsler, Chem. Mater. 19 (2007) 1062–1069.

[9] L.-S. Zhong, J.-S. Hu, Z.-M. Cui, L.-J. Wan, W.-G. Song, Chem. Mater. 19 (2007) 4557–4562.
[10] E. Antolini, Appl. Catal. B: Environ. 88 (2009) 1–24.
[11] J.P. Rolland, B.W. Maynor, L.E. Euliss, A.E. Exner, G.M. Denison, J.M. DeSimone, J. Am. Chem. Soc. 127 (2005) 10096–10100.
[12] C.H. Ho, J. Tobis, C. Sprich, R. Thomann, J.C. Tiller, Adv. Mater. 16 (2004) 957–961.
[13] X. Chen, G. Wu, J. Chen, X. Chen, Z. Xie, X. Wang, J. Am. Chem. Soc. 133 (2011) 3693–3695.
[14] Z. Zhang, C. Shao, Y. Sun, J. Mu, M. Zhang, P. Zhang, Z. Guo, P. Liang, C. Wang, Y. Liu, J. Mater. Chem. 22 (2012) 1387–1395.
[15] L. Shang, T. Bian, B. Zhang, D. Zhang, L.Z. Wu, C.H. Tung, Y. Yin, T. Zhang, Angew. Chem. Int. Ed. 126 (2014) 254–258.
[16] X. Li, D. Wang, G. Cheng, Q. Luo, J. An, Y. Wang, Appl. Catal. B: Environ. 81 (2008) 267–273.
[17] S.O. Obare, N.R. Jana, C.J. Murphy, Nano Lett. 1 (2001) 601–603.
[18] K. Kamata, Y. Lu, Y. Xia, J. Am. Chem. Soc. 125 (2003) 2384–2385.
[19] C. Li, J. Mei, S. Li, N. Lu, L. Wang, B. Chen, W. Dong, Nanotechnology 21 (2010) 245602.
[20] M. Oezaslan, M. Heggen, P. Strasser, J. Am. Chem. Soc. 134 (2011) 514–524.
[21] D. Li, S. Wu, Q. Wang, Y. Wu, W. Peng, L. Pan, J. Phys. Chem. C 116 (2012) 12283–12294.
[22] N. Sahiner, H. Ozay, O. Ozay, N. Aktas, Appl. Catal. B: Environ. 101 (2010) 137–143.
[23] M. Cattech, Cattle 6 (2002) 102–115.
[24] A. Corma, H. Garcia, Chem. Soc. Rev. 37 (2008) 2096–2126.
[25] P. Hu, J.V. Morabito, C.-K. Tsung, ACS Catal. 4 (2014) 4409–4419.
[26] J. Zhu, T. Wang, X. Xu, P. Xiao, J. Li, Appl. Catal. B: Environ. 130 (2013) 197–217.
[27] I. Nongwe, G. Bepete, A. Shaikjee, V. Ravat, B. Terfassa, R. Meijboom, N.J. Coville, Catal. Commun. 53 (2014) 77–82.
[28] J. Chen, Z. Xue, S. Feng, B. Tu, D. Zhao, J. Colloid Interface Sci. 429 (2014) 62–67.
[29] Y.-L. Shi, T. Asefa, Langmuir 23 (2007) 9455–9462.
[30] J. Qi, X. Dang, P.T. Hammond, A.M. Belcher, ACS Nano 5 (2011) 7108–7116.
[31] S. Raj, P. Rai, S.M. Majhi, Y.-T. Yu, J. Mater. Sci.: Mater. Electron. 25 (2014) 1156–1161.
[32] P.Z.L. Zhao, L.Y. Zhang, S.J. Bao, C.M. Li, Appl. Catal. B: Environ. 174 (2015) 361–366.
[33] P. Zheng, W. Zhang, J. Catal. 250 (2007) 324–330.
[34] H. Wang, J. Shen, Y. Li, Z. Wei, G. Cao, Z. Gai, K. Hong, P. Banerjee, S. Zhou, ACS Appl. Mater. Interfaces 5 (2013) 9446–9453.
[35] Y. Lu, Y. Yin, Z.-Y. Li, Y. Xia, Nano Lett. 2 (2002) 785–788.
[36] X. Sun, Y. Li, Angew. Chem. Int. Ed. 43 (2004) 597–601.
[37] T. Yang, J. Liu, Y. Zheng, M.J. Monteiro, S.Z. Qiao, Chem. Eur. J. 19 (2013) 6942–6945.
[38] Z. Wang, X. Chen, M. Chen, L. Wu, Langmuir 25 (2009) 7646–7651.
[39] S. Tang, S. Vongehr, X. Meng, J. Phys. Chem. C 114 (2009) 977–982.
[40] R. Ghosh Chaudhuri, S. Paria, Chem. Rev. 112 (2011) 2373–2433.
[41] X. Sun, Y. Li, Langmuir 21 (2005) 6019–6024.
[42] G.E. Lloyd, Mineral. Mag. 51 (1987) 3–19.
[43] L.-M. Chen, Y.-N. Liu, ACS Appl. Mater. Interfaces 3 (2011) 3091–3096.
[44] Y. Mi, W. Hu, Y. Dan, Y. Liu, Mater. Lett. 62 (2008) 1194–1196.
[45] P. Zhang, C. Shao, Z. Zhang, M. Zhang, J. Mu, Z. Guo, Y. Liu, Nanoscale 3 (2011) 3357–3363.
[46] R. Cui, C. Liu, J. Shen, D. Gao, J.J. Zhu, H.Y. Chen, Adv. Funct. Mater. 18 (2008) 2197–2204.
[47] A. Henricsson, U. Hedner, S.E. Bergentz, Thromb. Res. 12 (1978) 1099–1112.
[48] Q. Zhang, C.M. Cobley, J. Zeng, L.-P. Wen, J. Chen, Y. Xia, J. Phys. Chem. C 114 (2010) 6396–6400.
[49] C. Welch, C. Banks, A. Simm, R. Compton, Anal. Bioanal. Chem. 382 (2005) 12–21.
[50] N. Pradhan, A. Pal, T. Pal, Colloids Surf. A 196 (2002) 247–257.
[51] M.H. Rashid, T.K. Mandal, J. Phys. Chem. C 111 (2007) 16750–16760.
[52] Y. Chi, L. Zhao, Q. Yuan, X. Yan, Y. Li, N. Li, X. Li, J. Mater. Chem. 22 (2012) 13571–13577.